THE JOURNAL OF PROSTHETIC DENTISTRY

RESEARCH AND EDUCATION

Color stability, surface topography, and phase transformation of zirconia fabricated by additive and subtractive manufacturing after exposure to different artificial saliva formulations

Rafat Sasany, DDS, PhD,[a] Sultan Merve Uçar, DDS,[b] Miguel Gómez-Polo, DDS, MSc, PhD,[c] Marta Revilla-León, DDS, MSc, PhD,[d] and Seyed Ali Mosaddad, DDS[e]

Zirconia-based ceramics are widely used in restorative dentistry for their mechanical strength, biocompatibility, and esthetics.[1,2] Advances in subtractive (SM) and additive manufacturing (AM) have expanded their use in fixed prosthodontics,[3] enabling monolithic and multilayered restorations with varying translucency and composition.[2] While SM, typically involving milling presintered disks, is effective, it leads to material waste, limited surface detail, and potential microcracks.[4–7] AM offers greater design flexibility, reduced waste, and high accuracy,[7–16] though it may introduce surface irregularities and microstructural inconsistencies, affecting optical and mechanical performance.[7,10–14,17–20]

ABSTRACT

Statement of problem. How variations in salivary chemistry affect the long-term stability of additive manufacturing (AM) and subtractive manufacturing (SM) zirconia is unclear.

Purpose. The purpose of this in vitro study was to evaluate the effects of different salivary environments on the color stability, surface roughness, and phase transformation of zirconia fabricated by AM and SM.

Material and methods. Disk-shaped specimens (n=160) were fabricated from 4 zirconia materials: 2 AM—AMZ-LI (LithaCon 3Y, produced via lithography-based ceramic manufacturing [LCM]) and AMZ-IN (INNI Cera, produced via digital light processing [DLP])—and 2 SM—SMZ-ST (monolayer Katana ST) and SMZ-ML (multilayer Katana STML). Each material group was divided into 4 subgroups (n=10) based on the aging medium: distilled water (DW), neutral artificial saliva (AS7), acidic artificial saliva (AS4), or enzymatic artificial saliva containing α-amylase (ASE7). Surface roughness (Ra), color change (ΔE_{00}), and phase transformation were assessed. Data were analyzed using a 3-way repeated measures ANOVA with Tukey HSD or Bonferroni post hoc tests (α=.05).

Results. Ra was significantly affected by material type, aging condition, and fabrication method (all $P \leq .001$), with AMZ-LI and SMZ-ML maintaining the lowest Ra values (<0.60 µm) after aging. Color stability was similarly influenced ($P<.001$), with all groups remaining within clinically acceptable limits ($\Delta E_{00} \leq 1.8$). AMZ-LI (0.60 ±0.08 in DW; max=1.26) and SMZ-ML (0.84 ±0.05 in DW; max=1.20) showed the highest color stability, while SMZ-ST and AMZ-IN had higher ΔE_{00} in acidic and enzymatic media. Phase transformation was more pronounced in SM groups ($P<.05$), with SMZ-ML showing the greatest monoclinic increase, and AMZ-LI exhibiting the highest phase stability.

Conclusions. Both manufacturing techniques and aging environments significantly affected zirconia's surface, optical, and phase properties. AMZ-LI showed superior resistance to surface and phase degradation, while AMZ-LI and SMZ-ML exhibited the highest optical stability. (J Prosthet Dent 2026;135:157.e1-e10)

The authors declare that they have no known competing financial interests or personal relationships that could have appeared to influence the work reported in this paper.

[a]Associate Professor, Department of Prosthodontics, Faculty of Dentistry, Istanbul Biruni University, Istanbul, Turkey.
[b]Lecturer, Department of Prosthodontics, Faculty of Dentistry, Gelisim University, Istanbul, Turkey.
[c]Associate Professor, Department of Conservative Dentistry and Prosthodontics, School of Dentistry, Complutense University of Madrid (UCM), Madrid, Spain.
[d]Affiliate Assistant Professor, Graduate Prosthodontics, Department of Restorative Dentistry, School of Dentistry, University of Washington, Seattle, Wash.; Faculty and Director of Research and Digital Dentistry, Kois Center, Seattle, Wash.; and Adjunct Professor, Department of Prosthodontics, School of Dental Medicine, Tufts University, Boston, Mass.
[e]Researcher, Department of Conservative Dentistry and Bucofacial Prosthesis, Faculty of Odontology, Complutense University of Madrid (UCM), Madrid, Spain; and Adjunct Faculty Member, Department of Research Analytics, Saveetha Dental College and Hospitals, Saveetha Institute of Medical and Technical Sciences, Saveetha University, Chennai, India.

Clinical Implications

LCM-manufactured zirconia may offer enhanced long-term performance in patients with acidic or enzymatic saliva profiles.

Three mol% yttria-stabilized tetragonal zirconia polycrystal (3Y-TZP) zirconia became widely used as a metal-free structure because of its strength, but its opacity limited its anterior use to a substructure.[21] Veneering improved esthetics but often led to chipping from residual thermal stresses.[22,23] As a result, monolithic zirconia restorations remained popular, though initial formulations lacked translucency.[24] To address this, zirconia formulations with higher yttria content (4Y-, 5Y-PSZ) were introduced, offering improved translucency at the expense of flexural strength.[1,24,25] Multilayer systems were later developed to replicate natural dentition through gradual changes in translucency and chroma.[21,23,26,27] Despite strong performance in in vitro testing, their long-term behavior in the oral environment remains under study.

The oral cavity is a dynamic environment influenced by various physiological and behavioral factors. Among these, salivary pH plays a critical role, with fluctuations driven by diet, systemic health, and oral hygiene.[28] These pH variations can range from acidic levels (pH<5.5), as seen after consuming acidic beverages or in patients with xerostomia, to near-neutral or mildly alkaline conditions (pH 6.8 to 7.5),[28] considered physiological. Saliva composition may change under pathological conditions, such as in Sjögren's syndrome, promoting acidic and oxidative environments.[29] In addition to pH, enzymatic activity, particularly from α-amylase, may also modulate the chemical reactivity of saliva[30] and interact with restorative materials over time, contributing to pellicle formation and potential surface alterations.[30] This highlights the importance of simulating diverse oral conditions in laboratory studies,[31] where artificial saliva has commonly been used to replicate the effect of natural saliva.[32]

Despite zirconia's reputation for chemical stability, its long-term performance can be compromised by local factors, including exposure to saliva, temperature fluctuations, and pH variations.[33] Acidic media may increase surface roughness through grain boundary dissolution or softening, influenced by grain size and yttria content.[34] Increased roughness has been reported to impact plaque retention, wear behavior, and esthetic properties,[21,35–37] while surface irregularities and reflectivity changes promote extrinsic staining. Color stability, crucial for esthetic long-term success, is further challenged by exposure to staining agents like coffee, tea, and juices[38] and is influenced by surface finish, sintering, microstructure, and fabrication method.[2,39] Additionally, zirconia is prone to low-temperature degradation (LTD) under hydrothermal or acidic conditions,[13,14,40,41] involving tetragonal-to-monoclinic phase transformation with microcracking and surface damage that compromise strength, esthetics, and durability.[36,40,42–47]

Most in vitro studies have evaluated the effects of water or artificial saliva on the aging behavior of zirconia[36,42,48–50]; however, the specific impact of distinct and clinically relevant salivary environments, such as neutral saliva simulating physiologic conditions, acidic saliva mimicking pathological states including xerostomia or acid reflux, and enzymatic saliva reflecting the role of salivary proteins, remains poorly understood, particularly when comparing AM and SM methods. Furthermore, few investigations have simultaneously assessed mechanical surface properties and optical stability under such simulated conditions. Therefore, the present study aimed to evaluate the influence of neutral, acidic, and enzymatic salivary environments on the color stability, surface roughness, and phase composition of zirconia materials fabricated using AM and SM techniques. The research hypothesis was that both the composition of the aging medium and the fabrication method would significantly affect the material properties tested.

MATERIAL AND METHODS

A total of 160 disk-shaped zirconia specimens (Ø12×1.2 mm) were fabricated from 4 materials: 2 SM zirconia, monochromatic monolayer (Katana ST; SMZ-ST) and polychromatic multilayer (Katana STML; SMZ-ML) (Kuraray Noritake Dental Inc.); and 2 AM zirconia, LithaCon 3Y 210 (Lithoz GmbH; AMZ-LI) and INNI Cera (AON Co., Ltd.; AMZ-IN) (Table 1). All specimens were digitally designed using a software program (Meshmixer v3.5.474; Autodesk Inc) with an identical geometry to ensure consistency across groups, and the designs were exported in standard tessellation language (STL) format.

Specimens in the AMZ-LI group were fabricated from a 3Y-TZP ceramic slurry using a lithography-based ceramic manufacturing (LCM) 3D printer (CeraFab 7500; Lithoz GmbH). The STL design was imported into the printer's nesting software program, where build orientation and support structures were optimized for vertical printing with a 25-µm layer thickness. After printing, support structures were mechanically removed (6918B.HP.220 Diamond Disc; Komet), and the specimens were first cleaned with compressed air to eliminate loose particles. A final cleaning step was performed using a proprietary cleaning solution (LithaSol Spray;

Table 1. Zirconia material groups tested

Group	Brand	Manufacturer	Type	Manufacturing Method	Processing Technology	Yttria Content	Sintering Temperature (°C)	Layer Structure	Translucency Class	Color
AMZ-LI	LithaCon 3Y–210	Lithoz GmbH	Monochromatic	Additive	LCM	3Y-TZP	1550	Monolayer	NA	A2
AMZ-IN	INNI Cera	AON Co., Ltd.	Monochromatic	Additive	DLP	3Y-TZP	1530	Monolayer	NA	A2
SMZ-ST	Katana ST	Kuraray Noritake Dental Inc.	Monochromatic	Subtractive	Milling	3Y-TZP	~1550	Monolayer	High Translucency	A2
SMZ-ML	Katana STML	Kuraray Noritake Dental Inc.	Polychromatic	Subtractive	Milling	4Y-TZP	~1550	Multilayer	Super Translucent	A2

Translucency classes obtained from manufacturer data sheets.

3Y-TZP, 3 mol% yttria-stabilized tetragonal zirconia polycrystal; 4Y-TZP, 4 mol% yttria-stabilized tetragonal zirconia polycrystal; DLP, digital light processing; LCM, lithography-based ceramic manufacturing; NA, not applicable.

Lithoz GmbH) to ensure the complete removal of residual slurry and contaminants. The cleaned green bodies underwent a multistep thermal protocol: binder burnout was conducted at 1000 °C to eliminate organic components, followed by sintering at 1450 °C in a ceramic furnace (Programat CS4; Ivoclar AG).[51] The specimens were allowed to cool gradually to room temperature. Specimens in the AMZ-IN group were fabricated using a digital light processing (DLP) 3D printer (Zipro-D Bio-Ceramic 3D Printer; AON Co.) with build dimensions of 76.8×43.2×65 mm, a pixel resolution of 40 µm, and a layer thickness of 50 µm. After printing, the unpolymerized ceramic slurry was removed using approximately 200 ML of 83% ethanol through a combination of automated and manual cleaning protocols. The cleaned green bodies subsequently underwent a debinding process (Zirfur; AON Co, Ltd) at 1100 °C for 21 hours to eliminate organic components. Final sintering was performed in a high-temperature furnace (LHTCT; Nabertherm GmbH) at 1500 °C for 5 hours to achieve peak densification.[39] The same STL design was used to mill cylindrical specimens from presintered zirconia disks for the SMZ-ST and SMZ-ML groups using a 5-axis milling unit (Ceramill Motion 2; Amann Girrbach AG). The milled cylinders were then sectioned into 1.2-mm-thick disks using a water-cooled precision cutting saw (Vari/Cut VC-50; Leco Corp). After sectioning, all specimens were sintered in a ceramic furnace (Programat S1; Ivoclar AG) according to the manufacturer's recommended sintering schedules that included a heating rate of 10 °C/minute to a peak temperature of 1500 °C, a hold time of 2 hours, and controlled cooling to room temperature within the furnace.

Both surfaces of each disk specimen were mechanically polished using silicon carbide abrasive papers (Carbimet SiC; Buehler) in a sequential grit series (280, 400, 600, 800, 1000, and 1200) under water irrigation, with each grit applied for 120 seconds to ensure standardized surface preparation. Final polishing was completed using laboratory-grade zirconia polishing disks (Dialite ZR Polishers; Brasseler) until a consistent mirror-like finish was obtained. Specimens were subsequently cleaned in an ultrasonic bath containing 99% isopropyl alcohol for 5 minutes. Surface uniformity was verified under ×5 magnification to confirm the absence of irregularities or defects. After polishing, all specimens were measured using digital calipers (Absolute Digimatic; Mitutoyo; accuracy ±0.01 mm) to ensure that the final thickness remained within the target value of 1.2 mm. All laboratory procedures were carried out by a single experienced dental laboratory technician to ensure consistency.

Surface roughness (Ra, µm) was measured using a noncontact optical profilometer (Contour GT-K; Bruker) equipped with white-light interferometry. Each specimen was scanned along 3 horizontal and 3 vertical traces, each 5.5 mm in length and spaced 1 mm apart, using a cutoff length of 0.8 mm and a vertical resolution in the nanometer range. Measurements were made using a ×5 objective lens under ambient conditions. The arithmetic mean Ra for each specimen was calculated (Vision64; Bruker) as the average of all 6 traces.

Color coordinates (L*, a*, b*) were recorded using a spectrophotometer (CM-26d; Konica Minolta) equipped with an 8-mm aperture, D65 standard illuminant, and a 2-degree standard observer angle. Each measurement was repeated 3 times over 3 standardized backgrounds, black (L*=8.32, a*=0.43, b*=0.56), gray (L*=52.14, a*=−1.23, b*=−3.44), and white (L*=90.92, a*=−0.76, b*=8.79). A saturated sucrose solution was applied between the specimen and background surface to ensure consistent optical coupling and minimize refractive mismatch.[52] The device was calibrated before each measurement session using a white calibration tile provided by the manufacturer. Color change (ΔE_{00}) was calculated using the CIEDE2000 formula, which incorporates perceptual differences in lightness ($\Delta L'$), chroma ($\Delta C'$), and hue ($\Delta H'$), adjusted by the respective weighting functions (SL, SC, SH) and correction factors (kL, kC, kH), all set to 1.[53,54] The interaction between chroma and hue is further corrected by the RT term. The equation used was: $\Delta E_{2000}=\sqrt{\left(\frac{\Delta L'}{K_L \cdot S_L}\right)^2+\left(\frac{\Delta C'}{K_C \cdot S_C}\right)^2+\left(\frac{\Delta H'}{K_H \cdot S_H}\right)^2+R_T \cdot \left(\frac{\Delta C'}{K_C \cdot S_C}\right)\left(\frac{\Delta H'}{K_H \cdot S_H}\right)}$. Clinically perceptible and acceptable thresholds were set at $\Delta E_{00} \leq 0.8$ and ≤ 1.8.[55]

The phase composition of the specimens was evaluated using X-ray diffraction (XRD) analysis (D8 Advance; Bruker AXS GmbH), equipped with a Cu Kα radiation source (λ=1.5406 Å) and operated at 40 kV and 40 mA. Scans were performed over a 2θ range of 20 to 80 degrees, using a step size of 0.02 degrees and a scanning speed of 2 degrees per minute. Diffractograms were analyzed to assess the relative intensities of the tetragonal (t) and monoclinic (m) phases. Phase transformations were evaluated by comparing peak intensities before and after the aging protocol, with characteristic reflections corresponding to approximately 30.2 degrees for t(101), and 28.2 and 31.2 degrees for m(−111) and m (111), respectively.

Specimens were assigned to 4 storage media (n=10 per subgroup) simulating different oral environments, as summarized in Table 2: distilled water (neutral control; DW), artificial saliva at pH 7.0 (AS7), enzymatic artificial saliva containing α-amylase at pH 6.8 (ASE7), and acidic artificial saliva at pH 4.0 (AS4) (Fig. 1). The artificial saliva was prepared following the modified Macknight-Hane and Whitford formulation,[56] while the enzymatic solution was enriched with 100 units of α-amylase per 15 mL. Each specimen was immersed in 15 mL of the assigned medium, which was replaced every 48 hours throughout the aging period. To simulate thermal aging, all specimens underwent 5000 thermocycles between 5 °C and 55 °C (SD Mechatronik; Feldkirchen-Westerham). Each cycle included a 30-second dwell time in each temperature bath and a 10-second transfer interval according to the International Organization for Standardization (ISO) 11405 guidelines.[57] After completion of the aging procedures, surface roughness (Ra), color coordinates (L*, a*, b*), and phase composition were reevaluated using the same instruments and protocols described previously.

Statistical analysis was performed using a statistical software program (IBM SPSS Statistics, v29.0; IBM Corp). Data normality, variance homogeneity, and sphericity were assessed using the Shapiro–Wilk, Levene, and Mauchly tests, respectively, with Greenhouse–Geisser corrections applied when needed. A 3-way repeated measures ANOVA was used for surface roughness (Ra) and color change (ΔE_{00}), with “aging condition” as the within-subject factor and “material type” and “fabrication method” as between-subject factors; Tukey HSD (Ra) and Bonferroni (ΔE_{00}) tests were used for post hoc comparisons. For XRD phase transformation, a 3-way repeated measures ANOVA was applied with Bonferroni-adjusted pairwise comparisons. Effect sizes were calculated using partial eta-squared (η^2), considering $\eta^2>0.14$ as strong. Results are presented as mean ±standard deviation (SD). A priori power analysis (G*Power, version 3.1.9.7) indicated that 5 specimens per group provided 80% power at an effect size of f=0.4 and α=.05. All analyses were conducted by an independent, blinded biostatistician.

Table 2. Simulated oral environment groups used

Group Code	Medium Description	pH	Key Components / Purpose
DW	Distilled water	7.0	Negative control – neutral environment
AS7	Artificial saliva (chemical)	7.0	Electrolyte-based formulation simulating resting salivary chemistry
ASE7	Biorelevant enzymatic saliva	6.8	KCl, KSCN, $NaH_2PO_4 \cdot H_2O$, NaCl, NaOH, urea, α-amylase, uric acid, mucin, lysozyme
AS4	Acidic artificial saliva (Fusayama)	4.5	KCl, NaCl, $CaCl_2 \cdot 2H_2O$, $NaH_2PO_4 \cdot 2H_2O$, $Na_2S \cdot 9H_2O$, urea – simulates acidic pathological conditions

AS4, acidic artificial saliva; ASE7, enzymatic artificial saliva; AS7, artificial saliva at neutral pH 7.0; $CaCl_2 \cdot 2H_2O$, calcium chloride dihydrate; DW, distilled water; KCl, potassium chloride; NaCl, sodium chloride; $NaH_2PO_4 \cdot 2H_2O$, monosodium phosphate dihydrate; $Na_2S \cdot 9H_2O$, sodium sulfide nonahydrate; NaOH, sodium hydroxide.

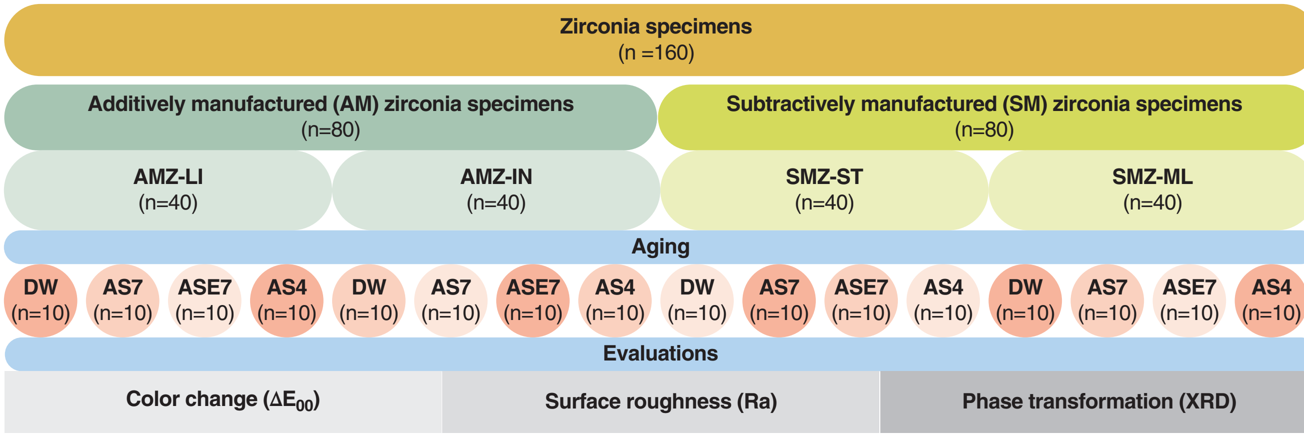

Figure 1. Study design and workflow, including fabrication methods, experimental grouping, aging protocols, and evaluation steps. AMZ-IN, additively manufactured zirconia (INNI Cera); AMZ-LI, additively manufactured zirconia (LithaCon); AS4, acidic artificial saliva; ASE7, enzymatic artificial saliva; AS7, artificial saliva at neutral pH 7.0; DW, distilled water; SMZ-ML, subtractively manufactured zirconia (multilayer, Katana STML); SMZ-ST, subtractively manufactured zirconia (monolayer, Katana ST).

RESULTS

Representative 3D surface topographies for each group are shown in Figure 2. All materials demonstrated a significant increase in Ra after thermocycling (P<.001). The 3-way repeated measures ANOVA revealed significant main effects of material type (F(3, 80)=38.24, P<.001), aging condition (F(4, 320)=41.07, P<.001), and fabrication method (F(2, 80)=9.12, P=.001), with a significant interaction between material type and aging condition (F(12, 320)=2.94, P=.017). Post hoc Tukey analysis indicated that SMZ-ST and AMZ-IN developed significantly rougher surfaces after aging in AS4 and AS7 media compared with AMZ-LI and SMZ-ML (P<.01). AMZ-LI and SMZ-ML maintained lower Ra values across all conditions (Table 3), with final roughness levels remaining below 0.60 µm.

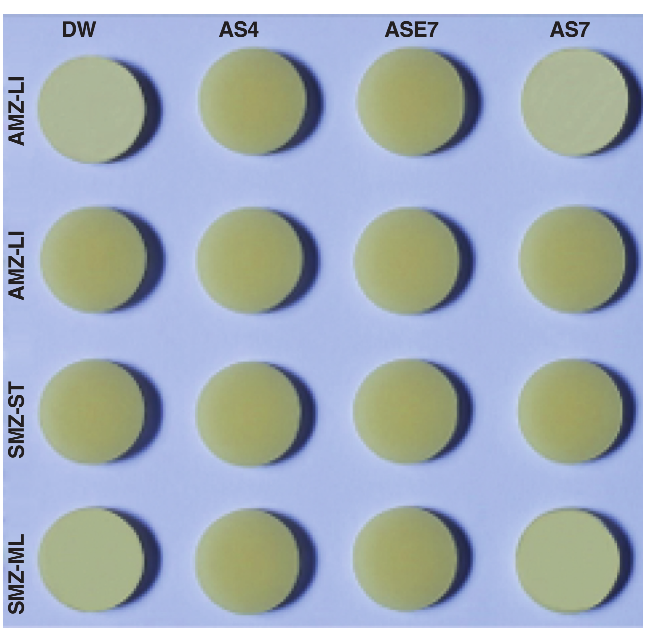

Figure 2. Representative 3D surface topography images of tested zirconia materials after thermocycling under different aging conditions. A, AMZ-IN (additively manufactured zirconia, INNI Cera); B, AMZ-LI (additively manufactured zirconia, LithaCon); C, SMZ-ML (subtractive multilayer zirconia, Katana STML); D, SMZ-ST (subtractive monolayer zirconia, Katana ST). AS4, acidic artificial saliva (pH 4.0); ASE7, enzymatic artificial saliva containing α-amylase (pH 6.8); AS7, artificial saliva at neutral pH 7.0; DW, distilled water.

The 3-way repeated measures ANOVA showed significant main effects of material type (F(3, 80)=42.51, P<.001), aging condition (F(4, 320)=36.72, P<.001), and fabrication method (F(2, 80)=7.39, P=.001) on ΔE_{00} values, along with a significant interaction between material type and aging condition (F(12, 320)=3.21, P=.014) (Table 4). Bonferroni post hoc analysis revealed that SMZ-ST and AMZ-IN exhibited significantly higher ΔE_{00} values in AS4 and ASE7 environments compared with AMZ-LI and SMZ-ML (P<.01). All zirconia groups demonstrated low ΔE_{00} values under all storage conditions. AMZ-LI showed the lowest ΔE_{00} values in distilled water (DW: 0.60 ±0.08) and maintained mild changes even in acidic and enzymatic environments (maximum ΔE_{00}=1.26). SMZ-ML demonstrated the lowest overall color changes across all aging conditions (maximum ΔE_{00}=1.20). In contrast, SMZ-ST and AMZ-IN exhibited significantly higher ΔE_{00} values under AS4 and ASE7 aging (Fig. 3).

Representative XRD patterns for all materials under different aging conditions are presented in Figure 4. Before aging, all specimens exhibited a predominant tetragonal (t) phase peak at approximately 30.2 degrees, with minimal or undetectable monoclinal (m) phase reflections at approximately 28.2 and 31.2 degrees, confirming initial phase stability. The 2-way repeated measures ANOVA showed that exposure to acidic and

Table 3. Surface roughness (Ra, µm) of zirconia specimens before and after thermocycling under different aging conditions (3-way repeated measures ANOVA, aging condition as within-subject factor; material type and fabrication method as between-subject factors)

Condition	AMZ-LI	AMZ-IN	SMZ-ST	SMZ-ML
Before TC	0.11 ±0.03[a]	0.19 ±0.02[a]	0.18 ±0.04[a]	0.12 ±0.01[a]
DW	0.19 ±0.03[a]	0.24 ±0.03[b]	0.25 ±0.02[b]	0.18 ±0.02[a]
AS4	0.57 ±0.06[b]	0.74 ±0.03[c]	0.80 ±0.05[c]	0.54 ±0.05[b]
ASE7	0.22 ±0.04[b]	0.35 ±0.03[b]	0.36 ±0.03[b]	0.26 ±0.03[a]
AS7	0.57 ±0.06[b]	0.77 ±0.03[c]	0.82 ±0.05[c]	0.60 ±0.05[c]

AMZ-IN, additively manufactured zirconia (INNI Cera); AMZ-LI, additively manufactured zirconia (LithaCon); AS4, acidic artificial saliva; ASE7, enzymatic artificial saliva; AS7, artificial saliva at neutral pH 7.0; DW, distilled water; Ra, arithmetic mean surface roughness; SMZ-ML, subtractively manufactured zirconia (multilayer, Katana STML); SMZ-ST, subtractively manufactured zirconia (monolayer, Katana ST); TC, thermocycling. Values with identical superscript letters indicate no significant difference (*P*>.05).

Table 4. Color stability (ΔE_{00}) of zirconia specimens before and after aging under different conditions (3-way repeated measures ANOVA, aging condition as within-subject factor; material type and fabrication method as between-subject factors)

Group	Before TC	DW	AS4	ASE7	AS7
AMZ-LI	0.57 ±0.03[a]	0.60 ±0.08[a]	1.26 ±0.09[b]	1.09 ±0.06[b]	1.24 ±0.08[b]
AMZ-IN	0.72 ±0.04[a]	0.98 ±0.09[b]	1.68 ±0.20[b]	1.24 ±0.07[b]	1.70 ±0.09[b]
SMZ-ST	0.94 ±0.02[b]	1.11 ±0.14[b]	1.70 ±0.14[b]	1.34 ±0.09[b]	1.80 ±0.05[c]
SMZ-ML	0.57 ±0.02[a]	0.84 ±0.05[b]	1.20 ±0.10[b]	1.00 ±0.05[b]	1.20 ±0.00[b]

AMZ-IN, additively manufactured zirconia (INNI Cera); AMZ-LI, additively manufactured zirconia (LithaCon); AS4, acidic artificial saliva; ASE7, enzymatic artificial saliva; AS7, artificial saliva at neutral pH 7.0; DW, distilled water; SMZ-ML, subtractively manufactured zirconia (multilayer, Katana STML); SMZ-ST, subtractively manufactured zirconia (monolayer, Katana ST); TC, thermocycling. Different superscript letters within a column indicate statistically significant differences between materials under the same aging condition (*P*<.05).

enzymatic saliva significantly increased tetragonal-to-monoclinic (t→m) transformation, particularly in SMZ-ML and SMZ-ST (*P*<.05). This was evidenced by increased intensities of the m(−111) and m(111) peaks after AS4 and ASE7 aging. AMZ-LI showed the highest resistance to phase transformation, retaining a significantly greater proportion of the tetragonal phase across all conditions (*P*<.05). SMZ-ML showed the highest increase (*P*<.05) in monoclinic content (Table 5).

DISCUSSION

The results of this in vitro study confirmed the research hypothesis, as both the manufacturing technique and chemical aging conditions significantly influenced the color stability, surface roughness, and phase transformation behavior of zirconia materials. Among the tested groups, both multichromatic (SMZ-ML) and AM zirconia using LCM (AMZ-LI) demonstrated excellent color stability, with ΔE_{00} values consistently below the clinical acceptability threshold (1.8) under all aging conditions, supporting the findings of Rigos et al,[51] who reported no significant ΔE differences between 3D printed and milled zirconia after aging in staining solutions. SMZ-ML showed the lowest maximum ΔE_{00} values across all media, indicating strong resistance to discoloration under chemical and thermal stress,[58] likely attributable to its intrinsic pigmentation throughout the multilayer structure and controlled yttria gradient, which improves shade stability and light scattering.[2,17,27] In contrast, AMZ-LI maintained the lowest baseline and distilled water ΔE_{00} values, remaining below the perceptibility threshold (0.8) in neutral conditions. Its acceptable color stability under acidic (1.26) and enzymatic (1.09) conditions may be linked to the higher-resolution LCM process (25-µm layers), refined slurry composition, and optimized light-polymerization, resulting in enhanced microstructural uniformity.[17–19] Conversely, AMZ-IN, fabricated using a DLP-based method, exhibited significantly higher ΔE_{00} values after aging in AS4 and ASE7,[20] nearing or reaching the clinical acceptability threshold. This may reflect the coarser layer thickness (50 µm), increased interlayer heterogeneity, and potential residual porosity associated with incomplete slurry removal.[45–47] These findings were consistent with those of Sabatini et al,[13] who highlighted the influence of build orientation and postprocessing on stain susceptibility in AM zirconia. SMZ-ST also showed elevated ΔE_{00} values, particularly under acidic conditions, likely due to its monochromatic composition and susceptibility to t→m phase transformation. These findings underscore how microstructural differences imposed by fabrication methods can translate into clinically relevant variations in optical performance.

Surface topography analysis confirmed that degradation was both material- and condition-dependent. While SMZ-ML and AMZ-LI retained more homogeneous surfaces, AMZ-IN and SMZ-ST exhibited more pronounced irregularities, particularly under acidic and

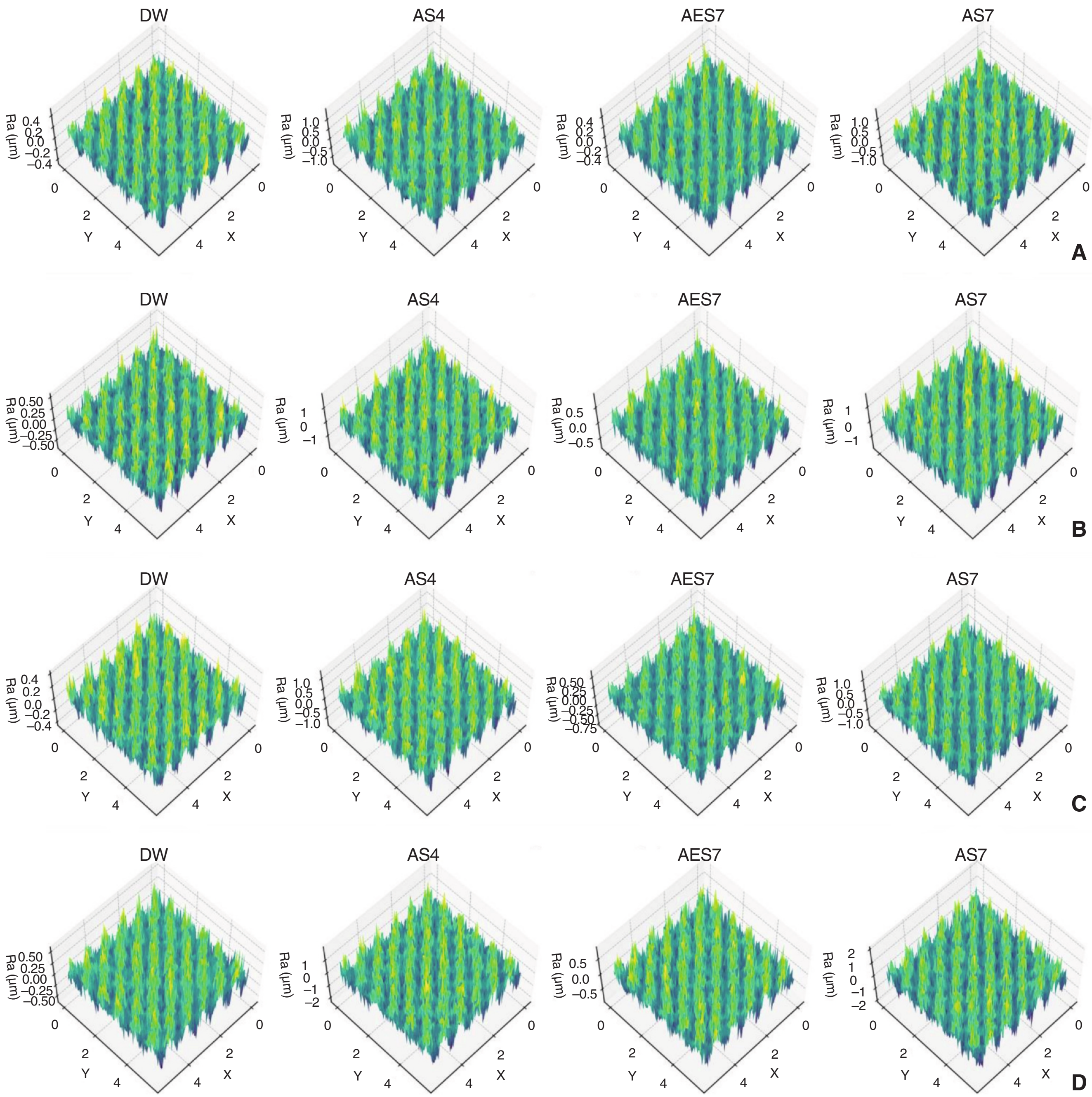

Figure 3. Representative specimens from each zirconia group after aging in different artificial saliva media. AMZ-IN, additively manufactured zirconia (INNI Cera); AMZ-LI, additively manufactured zirconia (LithaCon); AS4, acidic artificial saliva; ASE7, enzymatic artificial saliva; AS7, artificial saliva at neutral pH 7.0; DW, distilled water; SMZ-ML, subtractively manufactured zirconia (multilayer, Katana STML); SMZ-ST, subtractively manufactured zirconia (monolayer, Katana ST).

thermally stressed conditions. This is reflected in the Ra values and 3D profilometry maps, suggesting that lower grain cohesion and structural anisotropy in AMZ-IN increase its vulnerability to aging.[13,14,41] Moreover, the absence of pigmentation gradients in SMZ-ST may have left it more susceptible to surface etching and roughening. Phase transformation analysis further demonstrated that subtractive groups (SMZ-ST and SMZ-ML) were more prone to tetragonal-to-monoclinic (t→m) transformation, especially after exposure to pH 4 and enzymatic media. This finding was consistent with Chevalier's description of LTD[22] and supports previous studies[33,40] reporting that presintered, partially stabilized zirconia was particularly sensitive to hydrothermal and acidic stress. In contrast, AMZ-LI exhibited the highest phase stability, retaining a higher proportion of the

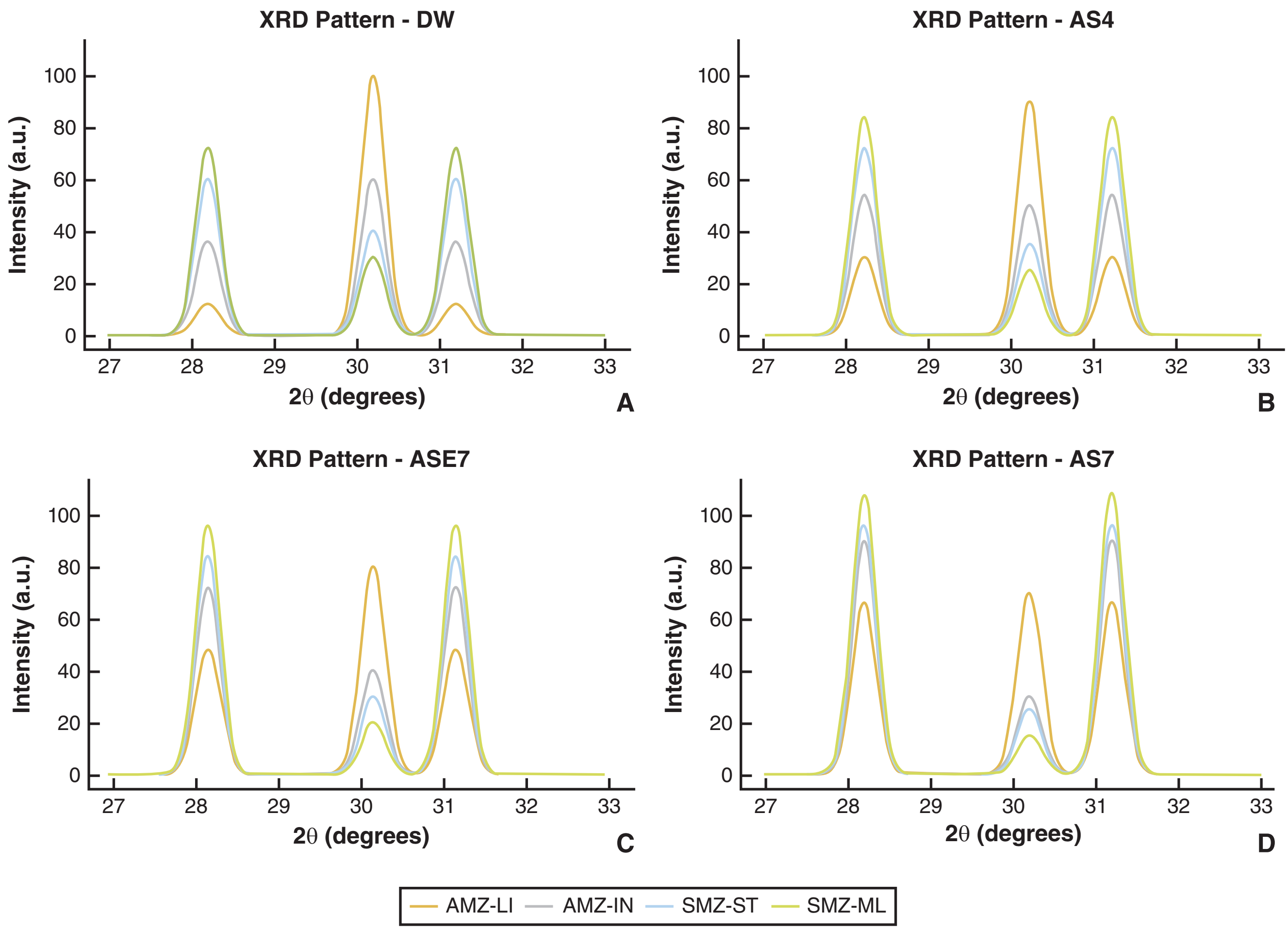

Figure 4. Phase transformation behavior of zirconia specimens after exposure to different aging conditions. A, AS4 (acidic artificial saliva, pH 4.0); B, ASE7 (enzymatic artificial saliva containing α-amylase, pH 6.8); C, AS7 (artificial saliva at neutral pH 7.0); D, DW (distilled water). AMZ-IN, additively manufactured zirconia (INNI Cera); AMZ-LI, additively manufactured zirconia (LithaCon); SMZ-ML, subtractively manufactured zirconia (multilayer, Katana STML); SMZ-ST, subtractively manufactured zirconia (monolayer, Katana ST).

Table 5. Monoclinic phase content (%) of zirconia specimens before and after aging under different conditions (2-way repeated measures ANOVA, aging condition as within-subject factor; material type as between-subject factor)

Group (Material)	Before	After DW	After AS4	After ASE7	After AS7
AMZ-LI	0.65 ±0.05[A]	2.10 ±0.12[a]	2.50 ±0.15[a]	2.90 ±0.14[a]	2.30 ±0.13[a]
AMZ-IN	0.89 ±0.06[A]	2.50 ±0.14[a]	3.40 ±0.16[b]	3.60 ±0.15[b]	2.80 ±0.14[a]
SMZ-ML	1.70 ±0.08[B]	3.30 ±0.16[b]	4.60 ±0.18[c]	4.80 ±0.17[c]	3.30 ±0.15[b]
SMZ-ST	1.50 ±0.07[B]	3.60 ±0.17[b]	4.40 ±0.19[c]	4.80 ±0.18[c]	3.60 ±0.16[b]

AMZ-IN, additively manufactured zirconia (INNI Cera); AMZ-LI, additively manufactured zirconia (LithaCon); AS4, acidic artificial saliva; ASE7, enzymatic artificial saliva; AS7, artificial saliva at neutral pH 7.0; DW, distilled water; SMZ-ML, subtractively manufactured zirconia (multilayer, Katana STML); SMZ-ST, subtractively manufactured zirconia (monolayer, Katana ST).

Before and after values represent percentage of monoclinic phase present as calculated from XRD analysis. Values are mean ±SD. Uppercase letters compare baseline values between materials; lowercase letters compare aging conditions within same material (α=.05).

tetragonal phase, possibly associated with the dense particle packing, lower defect concentration, and uniform sintering kinetics afforded by its LCM process.[12,16] Although previous studies[21,23] have shown that increasing the cubic phase enhances translucency at the expense of transformation toughening, the current findings suggest that optimized AM protocols, particularly those involving LCM, may strike a more favorable balance between esthetics and durability, challenging traditional assumptions about AM zirconia's structural limitations.[9,21]

From a clinical perspective, these findings suggest that not all AM zirconia are equivalent; LCM-produced zirconia may offer better durability in acidic or enzyme-rich oral environments compared with DLP-based alternatives. The findings emphasize the importance of simulating aggressive salivary environments, as pH 4 and enzymatic saliva, mimicking conditions such as xerostomia, Sjögren's syndrome, and acid reflux, intensified surface degradation and phase instability, justifying their inclusion in aging protocols.[29,32] Despite these findings, several limitations must be considered. First, the in vitro model did not replicate intraoral mechanical forces, salivary flow, or microbial activity. Second, only 2 AM systems and corresponding sintering protocols were evaluated.[4,8,9] Third, while artificial saliva formulations were selected to simulate different physiological conditions, they may not have fully replicated the biochemical complexity of pathological environments.[29,31,32] Lastly, aging was limited to thermocycling and immersion protocols.

CONCLUSIONS

Based on the findings of this in vitro study, the following conclusions were drawn:

1. Surface roughness, color stability, and phase transformation were significantly affected by both zirconia composition and aging environment.
2. SMZ-ML and AMZ-LI demonstrated the lowest color change values, while AMZ-LI exhibited the lowest surface roughness and highest phase stability.
3. Acidic and enzymatic artificial saliva accelerated surface degradation and tetragonal-to-monoclinic phase transformation.

REFERENCES

1. Cesar PF, Miranda RBP, Santos KF, et al. Recent advances in dental zirconia: 15 years of material and processing evolution. *Dent Mater*. 2024;40:824–836.
2. Abounassif FM, Alfaraj A, Gadah T, et al. Color stability of precolored and extrinsically colored monolithic multilayered polychromatic zirconia: Effects of surface finishing and aging. *J Prosthodont* 2024.
3. Mosaddad SA, Peláez J, Panadero RA, et al. Do 3D printed and milled tooth-supported complete monolithic zirconia crowns differ in accuracy and fit? A systematic review and meta-analysis of in vitro studies. *J Prosthet Dent*. 2025;133:383–393.
4. Moon JM, Jeong CS, Lee HJ, et al. A comparative study of additive and subtractive manufacturing techniques for a zirconia dental product: An analysis of the manufacturing accuracy and the bond strength of porcelain to zirconia. *Materials (Basel)*. 2022;15:5398.
5. Papadiochou S, Pissiotis AL. Marginal adaptation and CAD-CAM technology: A systematic review of restorative material and fabrication techniques. *J Prosthet Dent*. 2018;119:545–551.
6. Zeltner M, Sailer I, Mühlemann S, et al. Randomized controlled within-subject evaluation of digital and conventional workflows for the fabrication of lithium disilicate single crowns. Part III: marginal and internal fit. *J Prosthet Dent*. 2017;117:354–362.
7. Lyu J, Yang X, Li Y, et al. Dimensional accuracy and clinical adaptation of monolithic zirconia crowns fabricated with the nanoparticle jetting technique. *J Prosthet Dent*. 2024;132:985. .e1–.e7.
8. Floriani F, Henprasert P, Cho SH, Zandinejad A. Evaluating dimensional accuracy of additively manufactured zirconia and the impact of porosity variations: Part 2. *J Prosthet Dent*. 2025;134:228. .e1–.e6.
9. Zhang X, Wu X, Shi J. Additive manufacturing of zirconia ceramics: A state-of-the-art review. *J Mater Res Technol*. 2020;9:9029–9048.
10. Wang W, Sun J. Dimensional accuracy and clinical adaptation of ceramic crowns fabricated with the stereolithography technique. *J Prosthet Dent*. 2021;125:657–663.
11. Wang W, Yu H, Liu Y, et al. Trueness analysis of zirconia crowns fabricated with 3-dimensional printing. *J Prosthet Dent*. 2019;121:285–291.
12. Sasany R, Ucar SM, Mosaddad SA, Rodríguez Alonso V. Effect of polydopamine surface treatment on the mechanical properties of zirconia and resin occlusal veneers fabricated using additive and subtractive manufacturing: An in vitro study. *J Dent*. 2025;159:105805.
13. Sabatini GP, Çakmak G, Kahveci Ç, et al. Surface roughness, stainability, and translucency of additively manufactured zirconia with different build orientations and firing processes after coffee thermocycling. *J Prosthet Dent*. 2025;134:830.e1–830.e8.
14. Kessler A, Reichert T, Lindner S, et al. Influence of additive and subtractive zirconia and lithium disilicate manufacturing on tensile bond strength and surface topography. *J Prosthet Dent*. 2024;132:623. .e1–.e7.
15. Khanlar LN, Salazar Rios A, Tahmaseb A, Zandinejad A. Additive manufacturing of zirconia ceramic and its application in clinical dentistry: A review. *Dent J*. 2021;9:104.
16. Zenthöfer A, Fien D, Rossipal J, et al. Fracture resistance of 3D-printed occlusal veneers made from 3Y-TZP zirconia. *Materials (Basel)*. 2024;17:2122.
17. Ruggiero MM, Souza LVS, Magno MB, et al. Is additive manufacturing of dental zirconia comparable to subtractive methods when considering printing orientation and layer thickness? A systematic review and meta-analysis. *J Esthet Restor Dent* 2025.
18. Harrer W, Schwentenwein M, Lube T, Danzer R. Fractography of zirconia-specimens made using additive manufacturing (LCM) technology. *J Eur Ceram Soc*. 2017;37:4331–4338.
19. Revilla-León M, Meyer MJ, Zandinejad A, Özcan M. Additive manufacturing technologies for processing zirconia in dental applications. *Int J Comput Dent*. 2020;23:27–37.
20. Branco AC, Silva R, Santos T, et al. Suitability of 3D printed pieces of nanocrystalline zirconia for dental applications. *Dent Mater*. 2020;36:442–455.
21. Zhang Y, Lawn BR. Novel zirconia materials in dentistry. *J Dent Res*. 2018;97:140–147.
22. Chevalier J. What future for zirconia as a biomaterial? *Biomaterials*. 2006;27:535–543.
23. Zhang Y. Making yttria-stabilized tetragonal zirconia translucent. *Dent Mater*. 2014;30:1195–1203.
24. Pjetursson BE, Sailer I, Makarov NA, et al. All-ceramic or metal-ceramic tooth-supported fixed dental prostheses (FDPs)? A systematic review of the survival and complication rates. Part II: Multiple-unit FDPs. *Dent Mater*. 2015;31:624–639.
25. Alqutaibi AY, Ghulam O, Krsoum M, et al. Revolution of current dental zirconia: A comprehensive review. *Molecules (Basel)*. 2022;27:1699.
26. Yousry M, Hammad I, Halawani ME, Aboushelib M. Translucency of recent zirconia materials and material-related variables affecting their translucency: A systematic review and meta-analysis. *BMC Oral Health*. 2024;24:309.
27. Kolakarnprasert N, Kaizer MR, Kim DK, Zhang Y. New multi-layered zirconias: Composition, microstructure and translucency. *Dent Mater*. 2019;35:797–806.
28. Loke C, Lee J, Sander S, et al. Factors affecting intra-oral pH - A review. *J Oral Rehabil*. 2016;43:778–785.
29. Piacenza Florezi G, Pereira Barone F, Izidoro MA, et al. Targeted saliva metabolomics in Sjögren's syndrome. *Clinics (Sao Paulo)*. 2024;79:100459.
30. Santos MJ, Correia E, Vilela A. Exploring the impact of α-amylase enzyme activity and pH on flavor perception of alcoholic drinks. *Foods*. 2023;12:1018.
31. da Silva Vaz Junior I, Lu S, Pinto AFM, et al. Changes in saliva protein profile throughout Rhipicephalus microplus blood feeding. *Parasit Vectors*. 2024;17:36.
32. Grutle LA, Holm HV, Kopperud HBM, Uhlig S. Validation of a human saliva model for the determination of leachable monomers and other chemicals from dental materials. *J Chromatogr B Analyt Technol Biomed Life Sci*. 2024;1236:124073.
33. Nowicka A, El-Maghraby HF, Švančárková A, et al. Corrosion and low temperature degradation of 3Y-TZP dental ceramics under acidic conditions. *J Eur Ceram Soc*. 2020;40:6114–6122.
34. Yang H, Yang S, Attin T, Yu H. Effect of acidic solutions on the surface roughness and microhardness of indirect restorative materials: A systematic review and meta-analysis. *Int J Prosthodont*. 2023;36:81–90.
35. Mundhe K, Jain V, Pruthi G, Shah N. Clinical study to evaluate the wear of natural enamel antagonist to zirconia and metal ceramic crowns. *J Prosthet Dent*. 2015;114:358–363.
36. Hammoudeh H, Carracho L, Beard C, Razzoog M. Effect of different surface and heat treatments on the surface roughness, crystallography, and phase composition of high translucency zirconia for monolithic restorations. *J Prosthet Dent*. 2024;131:164. .e1–.e11.
37. Badarneh A, Eun Choi JJ, Lyons K, et al. The effect of aging on the wear performance of monolithic zirconia. *Dent Mater*. 2022;38:e136–e146.
38. Eftekhar Ashtiani R, Beyabanaki E, Razmgah M, et al. Color stability of resin hybrid ceramic materials in comparison to zirconia-reinforced lithium silicate ceramic. *Front Dent*. 2023;20:37.

39. Çağlayan E, Sasany R, Bolat BN, et al. Optical properties of repaired additively manufactured resin composites and zirconia and subtractively manufactured ceramics: a comparative study of composite resins. *BMC Oral Health*. 2025;25:144.
40. Flinn BD, Raigrodski AJ, Singh A, Mancl LA. Effect of hydrothermal degradation on three types of zirconias for dental application. *J Prosthet Dent*. 2014;112:1377–1384.
41. Alghauli MA, Alqutaibi AY, Wille S, Kern M. The physical-mechanical properties of 3D-printed versus conventional milled zirconia for dental clinical applications: A systematic review with meta-analysis. *J Mech Behav Biomed Mater*. 2024;156:106601.
42. Hatanaka GR, Polli GS, Adabo GL. The mechanical behavior of high-translucent monolithic zirconia after adjustment and finishing procedures and artificial aging. *J Prosthet Dent*. 2020;123:330–337.
43. Inokoshi M, Shimizu H, Nozaki K, et al. Crystallographic and morphological analysis of sandblasted highly translucent dental zirconia. *Dent Mater*. 2018;34:508–518.
44. Reale Reyes A, Dennison JB, Powers JM, et al. Translucency and flexural strength of translucent zirconia ceramics. *J Prosthet Dent*. 2023;129:644–649.
45. Lüchtenborg J, Willems E, Zhang F, et al. Accuracy of additively manufactured zirconia four-unit fixed dental prostheses fabricated by stereolithography, digital light processing and material jetting compared with subtractive manufacturing. *Dent Mater*. 2022;38:1459–1469.
46. Su G, Zhang Y, Jin C, et al. 3D printed zirconia used as dental materials: A critical review. *J Biol Eng*. 2023;17:78.
47. Ruggiero MM, Lim CH, Giugliano TS, et al. Balancing strength and translucency: The role of microstructure in additive and subtractive dental zirconia. *Dent Mater*. 2025;41:690–698.
48. Phatphutthitham C, Niyatiwatchanchai B, Rujiraprasert P, et al. Effect of grinding and polishing protocols on surface roughness, flexural strength, and phase transformation of high-translucent 5 mol% yttria-partially stabilized zirconia. *Eur J Dent*. 2025;19:80–89.
49. Atalay Seçkiner P, Gönüldaş F, Akat B, et al. Investigation of phase transformation and fracture pattern as a result of long-term chewing simulation and static loading of reduced-diameter zirconia implants. *Materials (Basel)*. 2024;17:4719.
50. Wille S, Möller R, Kern M. Influence of shading on zirconia's phase transformation and flexural strength after artificial aging. *Dent Mater*. 2023;39:702.
51. Rigos AE, Kesterke MJ, Chen JH, et al. Optical stability of 3D-printed and milled zirconia after artificial aging and immersion in liquids: An in vitro study. *J Prosthodont* 2025.
52. Hashem D, Al-Taee LA, Mourad SI, et al. Influence of zirconia thickness and background color on color matching accuracy of monolithic zirconia restorations. *J Dent*. 2025;160:105922.
53. Luo MR, Cui G, Rigg B. The development of the CIE 2000 colour-difference formula: CIEDE2000. *Color Res Appl*. 2001;26:340–350.
54. Sharma G, Wu W, Dalal EN. The CIEDE2000 color-difference formula: Implementation notes, supplementary test data, and mathematical observations. *Color Res Appl*. 2005;30:21–30.
55. Paravina RD, Ghinea R, Herrera LJ, et al. Color difference thresholds in dentistry. *J Esthet Restor Dent*. 2015;27:S1–S9.
56. Levine MJ, Aguirre A, Hatton MN, Tabak LA. Artificial salivas: Present and future. *J Dent Res*. 1987;66:693–698. (Spec No).
57. Braga RR, Meira JB, Boaro LC, Xavier TA. Adhesion to tooth structure: A critical review of "macro" test methods. *Dent Mater*. 2010;26:e38–e49.
58. Tabatabaian F, Karimi M, Namdari M. Color match of high translucency monolithic zirconia restorations with different thicknesses and backgrounds. *J Esthet Restor Dent*. 2020;32:615–621.

Corresponding author:
Dr Seyed Ali Mosaddad
Department of Conservative Dentistry and Bucofacial Prosthesis
Faculty of Odontology
Complutense University of Madrid (UCM)
Plaza Ramón y Cajal, s/n
Ciudad Universitaria, Madrid 2804
SPAIN
Email: semosadd@ucm.es

CRediT authorship contribution statement

Rafat Sasany: Conceptualization, Methodology, Software, Formal analysis, Validation, Investigation, Resources, Data curation, Writing – review and editing, Visualization, Supervision, Project administration. **Sultan Merve Uçar:** Software, Formal analysis, Investigation, Data curation, Writing – original draft preparation. **Miguel Gómez-Polo:** Validation, Writing – review and editing, Formal analysis, Project administration. **Marta Revilla-León:** Validation, Writing – review and editing, Formal analysis, Project administration. **Seyed Ali Mosaddad:** Investigation, Writing – review and editing, Visualization.

https://doi.org/10.1016/j.prosdent.2025.09.021